ELSEVIER

Thermochimica Acta 269/270 (1995) 537–552

thermochimica acta

Heat capacity study of La_2NiO_4 and Pr_2NiO_4 ☆

M. Castro, R. Burriel *

Instituto de Ciencia de Materiales de Aagón, CSIC-Universidad de Zaragoza, 50009 Zaragoza, Spain

Received 30 December 1994; accepted 25 May 1995

Abstract

A calorimetric study of La_2NiO_4 and Pr_2NiO_4 has been carried out with adiabatic and ac calorimetry. Thermodynamic functions of both compounds have been calculated at rounded temperatures. Heat capacity anomalies corresponding to structural transitions from the low-temperature tetragonal $P4_2/ncm$ phase to the higher-temperature orthorhombic Bmab phase have been found at 56 K for La_2NiO_4 and at 121.2 K for Pr_2NiO_4. The three-dimensional magnetic ordering of the Ni ions produces a small peak in the heat capacity at 328 K annd 324 K, respectively, for both compounds in agreement with the expected low-dimensional behavior. No long-range order of Pr^{3+} has been detected down to 2 K. A broad excess heat capacity in Pr_2NiO_4 over the estimated lattice contribution was found to be due to the electronic energy levels of Pr^{3+}. An energy gap of around 50 K between the ground and the first-excited level with equal degeneracies has been deduced.

Keywords: Ac Calorimetry; Adiabatic calorimetry; Heat capacity; La_2NiO_4; Pr_2NiO_4; Schottky anomalies; Thermodynamic functions

1. Introduction

The discovery of high T_c superconductivity has promoted the study of physical properties of compounds with a structure and chemical composition similar to the high T_c superconductors. The series R_2NiO_4 (R = rare earth ion) has the crystallographic K_2NiF_4-type structure [1,2] like La_2CuO_4 that belongs to the first family to high T_c superconductors. The R_2NiO_4 compounds follow the same sequence of structural

* Corresponding author.

☆ Presented at the 6th European Symposium on Thermal Analysis and Calorimetry, Grado, Italy, 11–16 September, 1994.

SSDI 0040-6031(95)02545-6

transformations presented by the $(La, Ba)_2CuO_4$ system [3], going from the high-temperature tetragonal I4/mmm to the intermediate orthorhombic Bmab and the low-temperature tetragonal $P4_2/ncm$ phase and show similar magnetic properties, but they do not have superconducting behavior.

Both families present three-dimensional magnetic ordering of the 3d ions [4, 5] around room temperature and strong two-dimensional magnetic character with a high in-plane exchange interaction.

Neutron diffraction experiments [2] show coexistence of phases in La_2NiO_4 in a broad temperature range from 40 to 100 K indicating the first-order character of the low-temperature structural transition.

Intimate connexion between magnetic and structural features has been detected. The low-temperature tetragonal structure allows the existence of a ferromagnetic component along the c axis [6] creating a strong internal magnetic field which induces a nonzero magnetic moment in the Pr^{3+} sublattice. No long-range magnetic ordering of Pr^{3+} has been detected down to 1.5 K. Spin reorientation transitions in the temperature range from 40 to 115 K have also been reported in Pr_2NiO_4 [6].

Our heat capacity measurements of La_2NiO_4 and Pr_2NiO_4 can give a clear indication of the type of transitions and information about the underlying magnetic behavior. There is no estimate of crystal-field parameters or measurements of the crystal-field energy levels of Pr^{3+} to compare with our calorimetric results. Nevertheless, the energy gap between the ground state and the first-excited level of Pr^{3+} has been estimated.

2. Experimental

Nonstoichiometric black samples were prepared by solid state reaction, firing stoichiometric amounts of high purity R_2O_3 (R = La, Pr) and NiO in air at 1350°C with several intermediate regrindings. The ideal stoichiometry (brown color samples) was obtained by passing a hydrogen flow through the samples for several hours at around 583 K [1].

Adiabatic heat capacity measurements were made in a computerized adiabatic calorimeter operating in the range 5 K–350 K as described in Ref. [7]. The amount of sample used was around 3.5 g for each compound.

Ac heat capacity measurements have been performed in a commercial ac calorimeter from Sinku-Riko Company (model ACC-IVL). A slab-shaped sample of pressed powder of around 3 mg mass and 0.3 mm thick was used. From the signal frequency response at constant temperature, the selected frequency for the heating power coming from chopped light was 2 Hz and the typical scan rate ranged between 10 K h^{-1} and 30 K h^{-1}. The temperature oscillation was detected with a type K thermocouple and measured with a digital lock-in amplifier. The ac calorimetry has been used in the temperature range where high relaxation times were experienced in the adiabatic measurements. The relative accuracy is about 0.1%. Absolute values have been obtained by scaling the relative values to the adiabatic measurements in the common temperature range where lower relaxation times existed. For the Pr compound, the low-temperature measurements were extended down to 2 K.

3. Results and discussion

The heat capacities of La_2NiO_4 and Pr_2NiO_4 from 2 to 350 K are shown in Figs. 1 and 2, respectively. The adiabatic measurements of both compounds are tabulated in Tables 1 and 2 in chronological order. After smoothing with orthogonal polynomials, the thermodynamic functions have been calculated by appropriate integration of the hat capacity functions. Tables 3 and 4 list the thermodynamic functions calculated at rounded temperature intervals. In order to obtain the thermodynamic data from 0 K, the lower temperature values from the ac measurements have been used extrapolating T^3 law down to 0 K.

In both compounds the three-dimensional antiferromagnetic ordering of the Ni sublattice is detected with a small peak at 328 ± 1 K for La_2NiO_4 and 324 ± 1 K for Pr_2NiO_4, in agreement with neutron experiments and magnetic measurements that give 330 and 325 K, respectively [8, 9]. The anomalous entropy is $\Delta S \approx 0.01R$ in both cases, indicating that most of the magnetic entropy ($\Delta S = R \ln 3$) has been consumed in stronger two-dimensional magnetic interaction in the NiO_2 planes. The estimated magnetic heat capacity jump at T_N is expected to be $\Delta C_m(T_N) = 0.16R$ according to expression (1) of Ref. [7] and is comparable to the experimental peaks of $0.2R$ and $0.13R$ for the Pr and La compounds, respectively. A higher in-plane exchange

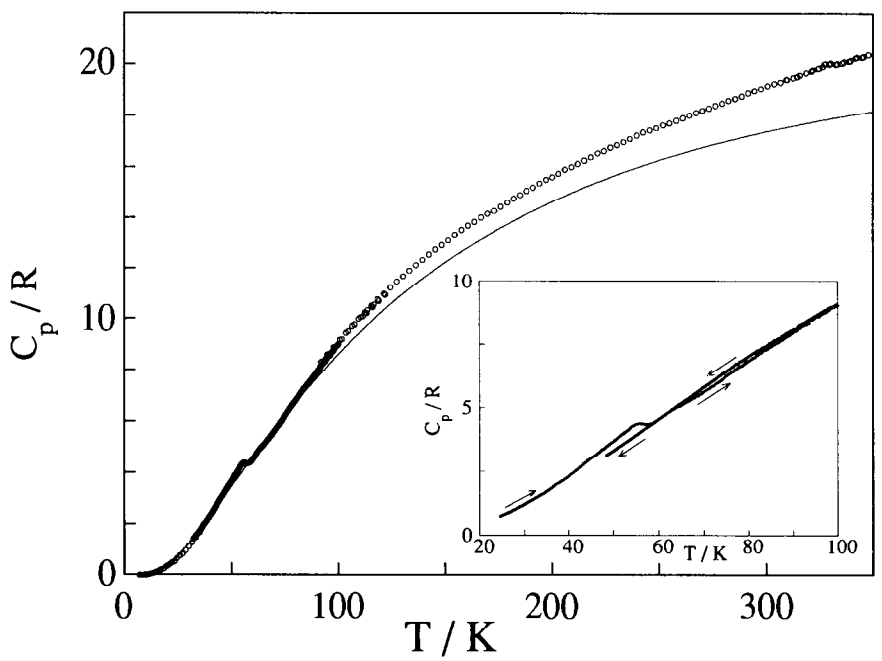

Fig. 1. Heat capacity measurements of La_2NiO_4. The lattice contribution, shown as a continuous line, has been calculated from the vibrational density of states as explained in Ref. [7]. The inset presents heating and cooling measurements through the structural transition.

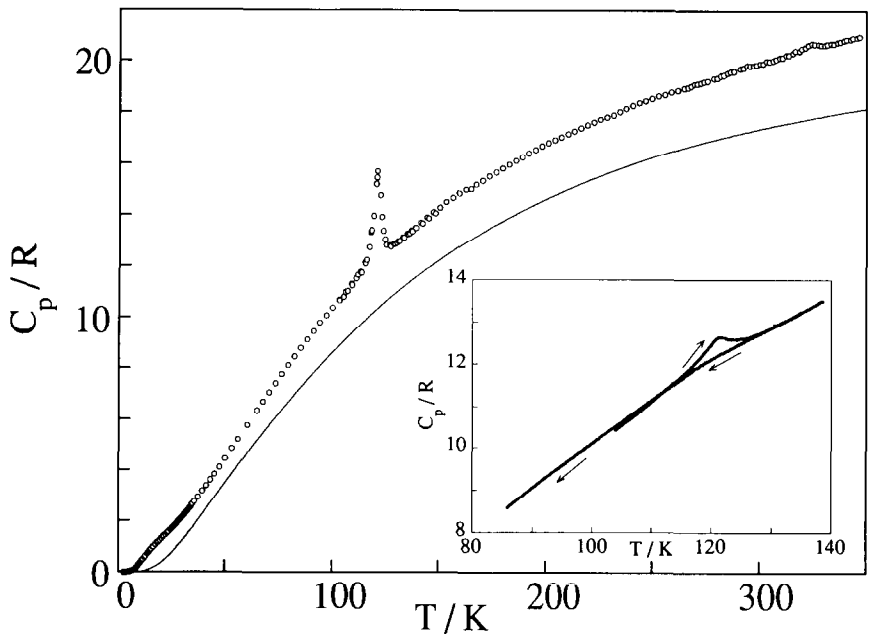

Fig. 2. Heat capacity measurements of Pr_2NiO_4. The continuous line corresponds to the calculated lattice contribution [7]. The inset manifests the hysteresis on cooling and heating runs through the structural transition from the orthorhombic to the low-temperature tetragonal structure.

Table 1
Adiabatic heat capacity data of La_2NiO_4

T/K	C_p/R
Series 1	
111.62	10.10
113.46	10.23
116.23	10.47
119.22	10.71
Series 2	
8.25	0.0131
9.79	0.0170
10.72	0.0260
11.77	0.0386
14.74	0.1195
Series 3	
11.28	0.0302

Table 1 (*Continued*)

T/K	C_p/R
12.45	0.0537
13.60	0.0825
14.76	0.1232
15.99	0.1629
17.25	0.2112
18.50	0.2567
19.72	0.3435
20.99	0.4158
22.30	0.4929
Series 4	
23.50	0.5405
24.61	0.6646
25.91	0.7685
27.23	0.8545
28.57	0.9789
Series 5	
30.10	1.135
31.78	1.304
33.55	1.493
Series 6	
91.72	8.342
94.68	8.625
97.65	8.911
100.62	9.197
103.61	9.474
106.59	9.738
109.59	10.00
112.58	10.25
115.57	10.52
118.57	10.77
121.58	11.00
124.58	11.24
Series 7	
127.52	11.48
130.46	11.70
133.47	11.92
136.49	12.13
139.50	12.36
142.52	12.56
145.54	12.76
148.57	12.95
151.59	13.12

Table 1 (*Continued*)

T/K	C_p/R
154.62	13.32
157.64	13.52
160.67	13.69
163.71	13.84
166.74	14.02
169.77	14.17
172.80	14.29
175.84	14.47
178.87	14.62
181.91	14.78
184.94	14.92
187.98	15.09
191.02	15.22
194.06	15.38
197.10	15.53
200.14	15.63
203.17	15.77
206.21	15.92
209.26	16.02
212.30	16.15
215.34	16.28
218.38	16.41
221.42	16.55
224.46	16.64
227.51	16.78
230.55	16.88
233.59	16.99
236.64	17.11
239.68	17.25
242.72	17.37
245.77	17.46
248.81	17.54
251.85	17.64
254.90	17.73
257.94	17.83
260.99	17.93
264.03	18.04
267.08	18.13
270.12	18.22
273.17	18.31
276.22	18.41
279.27	18.50
282.32	18.62
285.37	18.69
288.42	18.80
291.46	18.92
294.52	19.00
297.60	19.08

Table 1 (*Continued*)

T/K	C_p/R
300.67	19.19
303.72	19.27
306.77	19.32
309.82	19.44
312.86	19.50
315.91	19.61
318.96	19.70
322.01	19.81
325.05	19.87
328.10	20.05
Series 8	
309.34	19.43
321.42	19.76
324.47	19.86
327.51	20.03
330.56	20.06
333.61	20.04
336.67	20.11
339.72	20.16
342.77	20.29
345.83	20.32
Series 9	
314.69	19.55
326.79	19.93
329.84	20.02
332.88	20.02
335.94	20.07
338.99	20.13
342.04	20.26
345.09	20.29
348.15	20.39
Series 10	
92.74	8.370
95.72	8.651
98.70	8.940
101.68	9.233
104.66	9.539
107.65	9.781
110.65	10.07
113.64	10.33
116.64	10.56

Table 2
Adiabatic heat capacity data of Pr_2NiO_4

T/K	C_p/R
Series 1	
15.35	0.909
16.27	0.985
17.28	1.074
18.31	1.165
19.38	1.256
Series 2	
20.24	1.333
21.62	1.439
23.08	1.557
24.55	1.668
26.08	1.791
27.64	1.940
29.16	2.064
30.79	2.223
32.46	2.396
34.16	2.573
35.91	2.766
37.73	2.941
39.66	3.173
41.58	3.390
43.48	3.610
45.38	3.835
47.64	4.117
50.36	4.462
53.17	4.833
55.99	5.197
60.49	5.783
64.96	6.354
67.80	6.714
70.70	7.068
73.61	7.431
76.53	7.785
79.46	8.135
82.40	8.476
85.35	8.824
88.30	9.157
91.26	9.480
94.23	9.805
97.20	10.09
100.18	10.40
103.17	10.70
106.15	11.01
106.15	11.01
109.14	11.34
112.13	11.69

Table 2 (*Continued*)

T/K	C_p/R
115.11	12.17
118.05	13.33
120.91	15.47
123.96	13.39
127.15	12.82
130.21	12.92
133.24	13.10
136.26	13.29
139.28	13.50
142.31	13.68
145.33	13.88
148.36	14.08
Series 3	
103.39	10.68
105.23	10.81
107.25	11.05
109.27	11.28
111.28	11.54
113.29	11.79
115.30	12.12
117.29	12.75
119.25	13.97
121.17	15.71
123.21	13.93
125.35	12.84
127.42	12.77
129.45	12.88
131.47	12.98
133.50	13.12
135.52	13.25
137.55	13.37
Series 4	
113.92	11.76
115.93	12.26
120.64	15.21
122.63	14.78
124.75	13.06
128.91	12.88
130.94	12.98
132.97	13.13
135.01	13.29
137.04	13.41
139.08	13.51
141.46	13.72
144.34	13.91
147.39	14.12
150.44	14.30

Table 2 (*Continued*)

T/K	C_p/R
153.48	14.52
156.54	14.69
159.59	14.87
162.65	15.02
Series 5	
165.08	15.05
167.36	15.22
170.43	15.37
173.48	15.54
176.54	15.70
179.58	15.85
182.63	16.01
185.68	16.15
188.72	16.29
191.76	16.43
194.81	16.57
197.85	16.72
200.89	16.84
203.94	16.95
206.98	17.06
210.02	17.19
213.06	17.30
216.11	17.43
219.15	17.54
222.19	17.65
225.23	17.76
228.28	17.85
231.33	17.93
234.37	18.06
237.41	18.19
240.46	18.30
243.50	18.40
246.54	18.48
249.59	18.57
252.64	18.66
255.68	18.72
258.72	18.81
261.77	18.89
264.82	18.97
Series 6	
280.08	19.36
283.11	19.48
286.14	19.62
Series 7	
292.02	19.75
295.10	19.85

Table 2 (*Continued*)

T/K	C_p/R
298.18	19.89
301.25	19.93
304.30	20.02
307.35	20.10
Series 8	
310.29	20.17
313.27	20.27
316.30	20.43
319.35	20.53
322.39	20.66
325.44	20.70
328.49	20.66
331.55	20.70
334.61	20.72
337.65	20.81
340.71	20.89
343.76	20.94
346.81	21.00
Series 9	
266.49	19.00
269.51	19.12
272.55	19.18
275.59	19.24
278.63	19.35
281.67	19.46
284.72	19.56
287.77	19.63
290.82	19.73
293.86	19.86
296.92	19.85
299.97	19.94
303.02	20.03
306.07	20.05
309.12	20.16
312.16	20.26
315.21	20.35
318.26	20.43
321.20	20.58
324.24	20.72
327.28	20.69
330.34	20.66
333.39	20.73
336.45	20.78
339.50	20.85
342.55	20.90
345.60	20.96

Table 3
Calculated thermodynamic functions for La_2NiO_4 ($\Phi^\circ_m = \Delta_0^T S^\circ_m - \Delta_0^T H^\circ_m/T$)

T/K	$C^\circ_{p,m}/R$	$\Delta S^\circ_m/R$	$(\Delta H^\circ_m/R)$/K	Φ°_m/R
5	0.00065	0.00014	0.00059	0.00003
10	0.0179	0.0037	0.0306	0.0006
15	0.130	0.027	0.337	0.005
20	0.354	0.091	1.472	0.017
25	0.680	0.202	4.004	0.042
30	1.116	0.364	8.470	0.082
35	1.704	0.577	15.42	0.137
40	2.308	0.846	25.50	0.208
45	3.020	1.158	38.81	0.296
50	3.692	1.511	55.58	0.399
60	4.547	2.278	97.76	0.648
70	5.629	3.063	148.8	0.937
80	6.866	3.895	211.3	1.254
90	7.993	4.768	285.5	1.595
100	9.066	5.667	370.9	1.957
110	10.02	6.577	466.5	2.336
120	10.83	7.483	570.7	2.727
130	11.67	8.384	683.3	3.128
140	12.38	9.275	803.6	3.535
150	13.04	10.15	930.8	3.947
160	13.65	11.01	1064	4.362
170	14.16	11.86	1203	4.778
180	14.68	12.68	1348	5.194
190	15.18	13.49	1497	5.610
200	15.63	14.28	1651	6.024
210	16.06	15.05	1810	6.436
220	16.47	15.81	1972	6.845
230	16.87	16.55	2139	7.251
240	17.25	17.28	2310	7.653
250	17.59	17.99	2484	8.052
260	17.90	18.68	2661	8.448
270	18.22	19.36	2842	8.840
273.15	18.32	19.58	2900	8.962
280	18.52	20.03	3026	9.228
290	18.91	20.69	3213	9.612
298.15	19.14	21.22	3368	9.921
300	19.18	21.34	3403	9.991
310	19.44	21.97	3596	10.37
320	19.72	22.59	3792	10.74
330	20.04	23.20	3991	11.11
340	20.19	23.80	4192	11.47
350	20.41	24.39	4395	11.83

interaction constant ($J = -700$ K) does not enable the observation of this jump in La_2CuO_4 [4].

The peaks, detected at 56 ± 0.5 K for La_2NiO_4 and 121.2 ± 0.5 K for Pr_2NiO_4 upon heating, correspond to the low-temperature structural transition from the orthorhom-

Table 4
Calculated thermodynamic functions for Pr_2NiO_4 ($\Phi^\circ_m = \Delta_0^T S^\circ_m - \Delta_0^T H^\circ_m/T$)

T/K	$C^\circ_{p,m}/R$	$\Delta S^\circ_m/R$	$(\Delta H^\circ_m/R)$/K	Φ°_m/R
5	0.0366	0.0161	0.0564	0.0048
10	0.378	0.1150	0.8640	0.0280
15	0.879	0.3630	4.008	0.0950
20	1.311	0.6760	9.508	0.201
25	1.702	1.011	17.05	0.329
30	2.160	1.359	26.64	0.471
35	2.683	1.731	38.74	0.624
40	3.225	2.125	53.49	0.788
45	3.800	2.537	71.04	0.958
50	4.415	2.969	91.56	1.138
60	5.718	3.889	142.2	1.519
70	6.990	4.867	205.8	1.927
80	8.195	5.879	281.8	2.356
90	9.334	6.911	369.5	2.805
100	10.35	7.951	468.3	3.268
110	11.39	8.980	576.9	3.735
120	14.81	10.06	700.7	4.221
130	12.92	11.15	837.1	4.711
140	13.57	12.13	969.5	5.205
150	14.26	13.09	1109	5.696
160	14.88	14.04	1255	6.196
170	15.34	14.95	1406	6.679
180	15.88	15.84	1562	7.162
190	16.35	16.71	1723	7.641
200	16.79	17.56	1889	8.115
210	17.20	18.39	2059	8.585
220	17.56	19.20	2233	9.050
230	17.91	19.99	2410	9.512
240	18.27	20.76	2591	9.964
250	18.59	21.51	2775	10.41
260	18.84	22.25	2962	10.85
270	19.11	22.96	3152	11.29
273.15	19.20	23.19	3213	11.43
280	19.39	23.66	3345	11.71
290	19.71	24.35	3540	12.14
298.15	19.90	24.90	3702	12.48
300	19.93	25.02	3739	12.56
310	20.18	25.68	3939	12.97
320	20.55	26.33	4142	13.39
330	20.68	26.96	4349	13.78
340	20.86	27.58	4557	14.18
350	21.06	28.19	4766	14.57

bic Bmab to the tetragonal $P4_2/ncm$ phase associated with rotation of the NiO_6 octahedra. Similar anomalies and entropy contents have been detected in $La_{1.875-x}Nd_xSr_{0.125}CuO_4$ for the same kind of transition [10]. Anomalous high relaxation times for La_2NiO_4 in the temperature range from 30 to 80 K indicate a phase

coexistence in this range, in agreement with a neutron diffraction study [2]. The temperature-dependence of the relaxation time, after a heat pulse, has been plotted in Fig. 3. A clear strong increase starts at around 80 K with a maximum at 50 K and, then, decreases at lower temperatures. This large stabilization time can indicate a continuous conversion between the two phases.

Thermal hysteresis has been observed by ac calorimetry. Cooling and heating runs have been performed between 80 and 300 K for the Pr compound. In the inset of the Fig. 2, both runs are shown in the temperature range from 85 and 140 K. On heating, a peak appears at the temperature of the sharp adiabatic peak corresponding to the structural phase transition but, on cooling, no anomaly has been detected down to 85 K indicating the presence of thermal hysteresis. Further heating from 85 K again shows a peak at the same temperature. The different shape of the peaks obtained from adiabatic and ac calorimetry are due to the phase coexistence and the limitations of the ac technique for first-order transitions; latent heats are not detected in the heat capacity signal with ac calorimetry. Similar behavior has been found in La_2NiO_4 since no anomaly appears down to 48 K on cooling, whereas on heating from 4.2 K a clear anomaly appears at 56 K as shown in the inset of Fig. 1.

The heat capacity of Pr_2NiO_4 shows a broad shoulder around 20 K. Pr^{3+} is a magnetic ion with a $^3H_4$ ground multiplet and total angular momentum $J = 4$. Due to the D_{4h} point symmetry of the Pr^{3+} site, the ground multiplet splits into two doublets and five singlets of different energies giving rise to Schottky anomalies. In order to

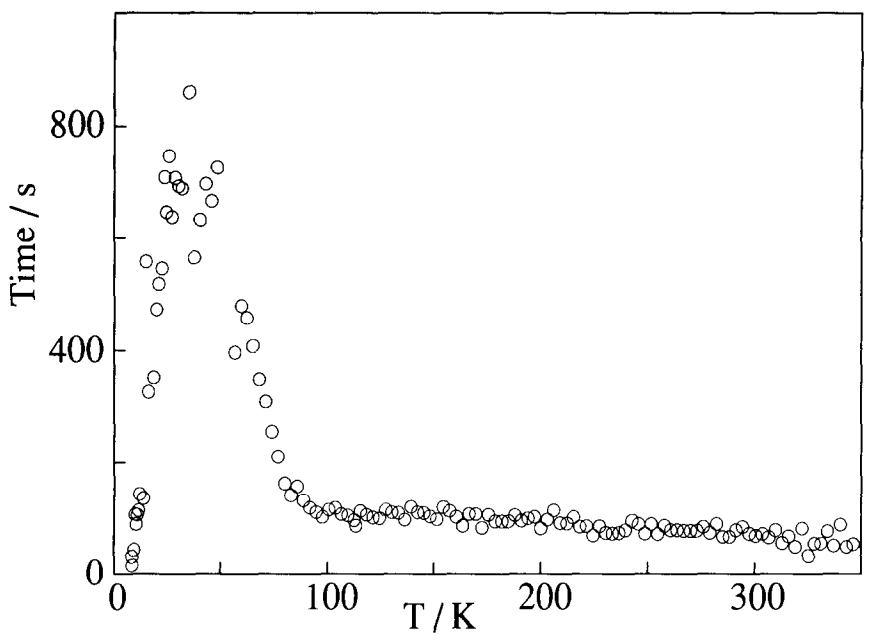

Fig. 3. Temperature-dependence of the relaxation time after a heat pulse for the sample of La_2NiO_4. The high values between 80 and 30 K correspond to the temperature region with phase coexistence.

obtain an estimate of the electronic energy levels and magnetic contribution of Pr^{3+} at low temperature, the lattice heat capacity, C_l, has to be evaluated. It has been calculated from the phonon density of states of La_2NiO_4 following the procedure given in Ref [7]. In Fig. 1, the calculated lattice heat capacity is shown as a continuous line and can be compared with the experimental La_2NiO_4 data. The excess, at temperatures higher than 90 K, could be attributed to the magnetic contributions from the Ni sublattice together with anharmonic terms and the difference in the lattice estimate due to the nonstoichiometric sample used for the phonon analysis. The equipartition limit of the heat capacity value, $21R$, is not reached in the experimental data despite such additive contributions.

The anomalous low-temperature heat capacity of Pr_2NiO_4, after subtracting the lattice contribution, is shown in Fig. 4. This excess value should correspond to the Schottky anomaly associated with the crystal-field splitting of the ground multiplet of Pr^{3+}. Reported spin reorientations of the Ni sublattice can also contribute to this excess [5, 6]. No peak has been detected down to 2 K, discounting any possibility of long-range ordering of the Pr^{3+} ions, in agreement with magnetic measurements [6]. The rounded anomaly with a maximum at 23 K in Fig. 4 must arise from the lowest electronic energy levels. Due to the lack of information about the crystal-field par-

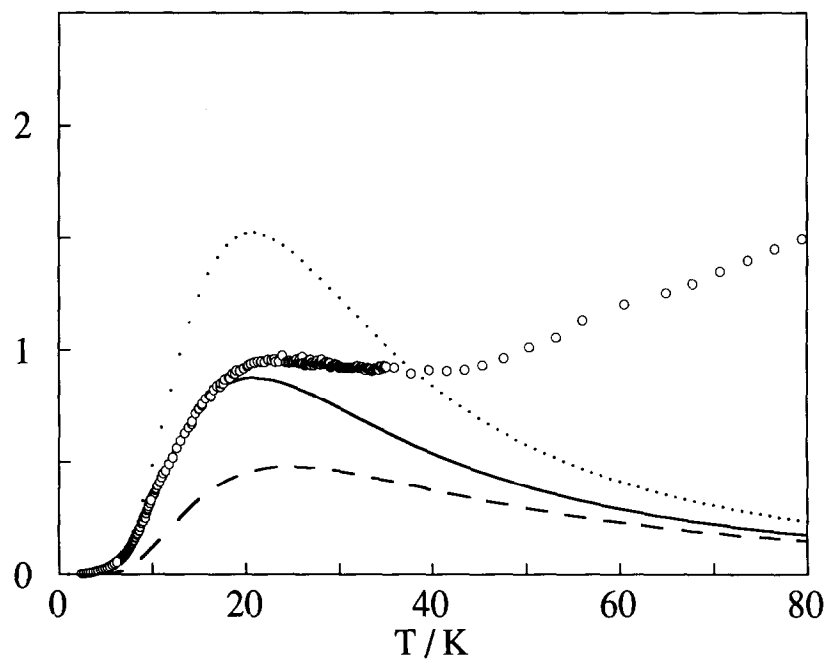

Fig. 4. Low-temperature heat capacity contribution of the Pr^{3+} energy levels deduced from the measured values (○). The dotted and dashed lines correspond to simple two-level models with degeneracy ratio equal to 2 and 0.5, respectively, and an energy gap of 55 K. The continuous line is the best fit for the low-temperature part of the anomaly corresponding to a degeneracy ratio equal to 1 and an energy gap of 50 K.

ameters and the absence of experimental measurements of the energy levels in Pr_2NiO_4, a direct comparison with our calorimetric results cannot be performed. Nevertheless, a calculation of the first-exited state can be obtained with a simple two-level model.

The maximum value and corresponding temperature of the anomalous heat capacity agrees with a Schottky function corresponding to a degeneracy ratio equal to 1 and an energy separation of 55 K between the ground state and the first-excited level. For ratios of 0.5 or 2, that would correspond to a doublet ground state and a singlet first-exited state or vice versa, the corresponding Schottky anomalies give too low or too high, values as indicated with the dashed and dotted curves of Fig. 4. The best fit for the low-temperature part of the anomaly is obtained for an energy gap of 50 K between a ground state and first-exited state with equal degeneracies. The continuous line in Fig. 4 corresponds to this Schottky anomaly. The influence of higher crystal-field levels give additional contributions at higher temperatures, but our heat capacity values do not enable a unique choice for the rest of the levels.

Acknowledgments

We thank F. Fernández and R. Saez-Puche, from the Universidad Complutense de Madrid (Spain), for providing the samples used in these measurements. This work has been supported by CICYT, Projects PB91-0652 and MAT94-0804.

References

[1] R. Saez-Puche, F. Fernández, J. Rodríguez-Carvajal and J.L. Martínez, Solid State Commun., 72 (1989) 273.
[2] J. Rodríguez-Carvajal, M.T. Fernández-Díaz and J.L. Martínez, J.Phys.: Condens. Matter, 3 (1991) 3215.
[3] J.D. Axe, A.H. Moudden, D. Hohlwein, D.E. Cox, K.M. Mohanty, A.R. Moodenbaugh and Y. Xu, Phys. Rev. Lett., 62 (1989) 2751.
[4] K. Sun, J.H. Cho, F.C. Chou, W.C. Lee, L.L. Miller, D.C. Johnston, Y. Hidaka and T. Murakami, Phys. Rev. B, 43 (1991) 239.
[5] X. Batlle, X. Obradors and B. Martínez, Phys. Rev. B, 45 (1992) 2830.
[6] M.T. Fernández-Díaz, J.L. Martínez, J. Rodríguez-Carvajal, J. Beille, B. Martínez, X. Obradors and P. Odier, Phys. Rev. B, 47 (1993) 5834.
[7] M. Castro and R. Burriel, Phase Transitions and Crystal-Field Levels in Nd_2NiO_4, Thermochim. Acta, (this issue).
[8] X. Batlle, X. Obradors, M.J. Sayagués, M. Vallet and J. González-Calbet, J. Phys.: Condens. Matter, 4 (1992) 487.
[9] M.T. Fernández-Díaz, J. Rodríguez-Carvajal, J.L. Martínez, G. Fillion, F. Fernández and R. Saez-Puche, Z. Phys. B, 82 (1991) 275.
[10] D.A. Wright, R.A. Fisher, N.E. Phillips, M.K. Crawford and E.M. McCarron III, Physica B, 194 (1994) 469.